Analysis and experiment of the film-soil separation mechanism of the residual film recovery machine in the plough layer

Shilong Shen[1,2], Jiaxi Zhang[1,2*], Yichao Wang[1,2], Zhenwei Wang[1,2], Jinming Li[1,2], Wenhao Dong[1,2]

(1. *College of Mechanical and Electrical Engineering, Xinjiang Agricultural University, Urumqi 830052, China*;
2. *Key Laboratory of Xinjiang Intelligent Agricultural Equipment, Urumqi 830052, China*)

Abstract: In order to solve the problems of unclear film separation in traditional topsoil residual film recovery machine and secondary broken film caused by the toot-shaped structure, a film-soil conveying and vibration separation device was designed. It mainly consists of a first-level vibration conveying chain, roller extrusion and crushing mechanism and secondary conveyor chain, which can complete the functions of conveying, vibration separation, and crushing separation of film-soil composite. Firstly, the mechanical model of the transport process of the film-soil composite was established, and the transport stability of the film-soil composite was analyzed. The vibration characteristics of the vibration mechanism were analyzed by analytical method, and the vibration model of the vibration mechanism was established. The distribution state of residual film-soil mixture was observed and measured by high-speed camera, and the influence of vibration wheel speed and installation distance on the distribution height of residual film-soil mixture was found out. The crushing mechanism of the residual film-soil composite was proved by studying the roller extrusion and crushing mechanism. The Box-Behnken response surface test method was used to carry out field tests on the transport and vibration separation device of film-soil with soil content rate and film leakage rate as evaluation indices. The results indicated that the influencing factors on the soil content rate in a dscending order are conveyor chain speed, vibration wheel speed, and installation distance. In contrast, the factors affecting the film leakage rate, also ranked from largest to smallest, are conveyor chain speed, installation distance, and vibration wheel speed. The combination of film-soil separation parameters is as follows: conveying chain speed is 1.6 km/h, vibration wheel speed is 189.7 r/min, installation distance is 769.7 mm, at this time the soil content rate is 18.31%, and the film leakage rate is 9.49%, which meet the requirements of the recovery of residual film in the plough layer. The conveying and vibration model established in this study can provide a theoretical basis and technical reference for elucidating the soil-film separation process.

Keywords: residual film, film-soil conveying and vibration separation device, film-soil composite, steady transportation, vibration mechanism, crushing mechanism, field tests

DOI: 10.25165/j.ijabe.20251805.9800

Citation: Shen S L, Zhang J X, Wang Y C, Wang Z W, Li J M, Dong W H. Analysis and experiment of the film-soil separation mechanism of the residual film recovery machine in the plough layer. Int J Agric & Biol Eng, 2025; 18(5): 181–190.

1 Introduction

Mulching technology is widely used in arid crop growing areas such as Xinjiang in China due to its excellent effect of conserving soil moisture and increasing soil yield[1-3]. At present, the area of mulch used in Xinjiang exceeds 3.67 million hm^2 and the use amount is 2.5×10^5 t, which is a huge amount of data[4]. With the increase of farmland film cover area year by year, the residual film that is not recovered in time accumulates in the soil. At present, there is farmland in Xinjiang that has not been harvested for ten years. According to statistics, at present, the average residual amount of mulching film in Xinjiang farmland is about 260 kg/hm^2, and the trend is constantly increasing[5-7]. Residual film has a great impact on soil physical and chemical properties and crop yield, which is not conducive to the sustainable use of agricultural land[8-10]. Previous studies found that the mechanical properties of the residual film were gradually reduced due to erosion by topsoil, rocks, water, and fertilizer[11-13]. Secondly, the residual film is soft and closely combined with the soil. It is generally spread or aggregated in the soil and distributed in the plough layer irregularly, which makes the separation of the film-soil difficult. In addition, the residual film distribution is fragmented, and the mechanical film leakage is generally serious[14].

Foreign farmland mainly uses highly reliable and high-intensity mulching technology, and the whole mulching film can be recovered after crop harvest, so there is no agricultural film retention problem in the plough layer. So far, there are few researches on soil residual film recovery technology in the world[15]. Chinese scholars' research on residue film recycling in the plough layer originated in the 1980s, and so far, different kinds of soil layer residue film recycling machines have been formed[16]. In view of different technical problems, Chinese scholars have developed different principles of film-soil separation structures for residual film recovery in the plough layer. For example, Zhang et al.[17] designed a reverse film-soil separation device through the different friction characteristics between residual film and soil clods on the friction belt, and transported the residual film to the collector, and the soil blocks fell to the field by gravity. Guo et al.[18] proposed a

Received date: 2025-03-19 **Accepted date:** 2025-06-27

Biographies: Shilong Shen, PhD Candidate, research interest: recycling agriculture technology and equipment, Email: 2505770715@qq.com; **Yichao Wang**, PhD, research interest: harvesting machinery, Email: 360318122@qq.com; **Zhenwei Wang**, PhD Candidate, research interest: recycling agriculture technology and equipment, Email: 995839254@qq.com; **Jinming Li**, PhD Student, research interest: recycling agriculture technology and equipment, Email: 1935347351@qq.com; **Wenhao Dong**, PhD Student, research interest: recycling agriculture technology and equipment, Email: 3221924804@qq.com.

***Corresponding author: Jiaxi Zhang**, PhD, Professor, research interest: recycling agriculture technology and equipment research. College of Mechanical and Electrical Engineering, Xinjiang Agricultural University, Urumqi 830052, China. Email: zhangjiaxi@xjau.edu.cn.

film-soil separation method in which the residual film in the plough layer is lifted by the film picking mechanism, and the residual film on the comb teeth is sucked into the collecting box. Luo et al.[19] developed a chaff screen type topsoil residual film recovery machine in which, after the soil is loosened by the digging shovel, the residual film hook in the soil layer is pulled out by the conveyor chain teeth to realize the separation of the film-soil. Zhang et al.[20] mainly used vibration structure to initially separate film and soil, and then inhaled the separated film into the aggregate box by fan.

A comparative analysis of current subsoil residual film recovery equipment developed by Chinese researchers and institutions shows that the prevailing soil-film separation mechanism primarily utilizes rake teeth to "hook and extract" the buried film from the soil, followed by pneumatic conveyance to transport the film from the teeth into a collection chamber. Due to prolonged burial in the subsoil layer, the film forms strong adhesive bonds with soil particles. During extraction, the rake teeth inevitably retrieve film fragments with attached soil clumps that resist removal, resulting in recovered film with high soil contamination levels. The tooth-based extraction systems (including both comb-type and spring-tooth designs) fail to adequately consider the mechanical properties of degraded film, frequently causing film fragmentation during the recovery process due to excessive tensile stresses[21]. The pneumatic film-soil separation mechanism will suck fine soil particles into the collecting film box while absorbing film, and increase the power consumption of the whole machine[22].

This study addresses the current status and operational requirements of agricultural film residue recovery in China, developing a "vibrating conveyor+roller extrusion+transportation" film-soil separation device suitable for the recovery of residual film from the plough layer in Xinjiang cotton fields. The device uses a two-stage conveyor chain combination for transporting film residues, which increases the length of film-soil transport and separation, ensuring more thorough separation. The roller mechanism crushes and breaks soil blocks that either wrap around the film residue or are adhered to its surface, enabling stable transportation of the plough layer film residue and the separation of the film-soil composite. This reduces the soil content rate and ensures the quality of film recovery from the plough layer. Based on this, the stability of film-soil transportation on the first-level conveyor chain is analyzed, and the effects of vibration mechanism parameters on the film-soil separation are explored. Furthermore, the performance of the film-soil composite during the breaking and separation process is studied, analyzing the extrusion and crushing mechanism. The study aims to conduct field tests of film-soil separation device with soil content rate and film leakage rate as the objectives, followed by further optimization of structural parameters to determine the optimal parameter ratio. This research seeks to provide a basis for achieving efficient film-soil separation for residual film recovery in the plough layer.

2 Overall design and working principle

The film-soil conveying and vibration separation device is shown in Figure 1. It contains a first-level conveyor chain, vibrating roller mechanism, a roller extrusion crushing mechanism, and a secondary conveyor chain.

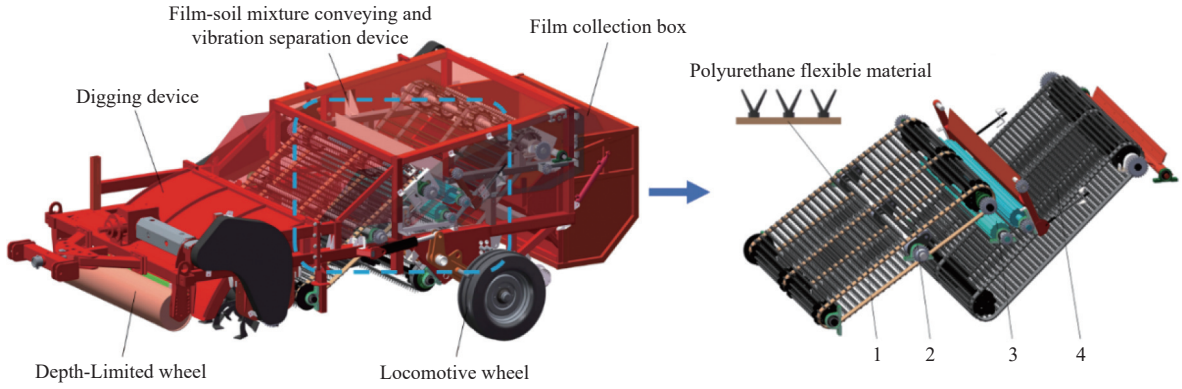

1. First-level conveyor chain 2. Vibrating roller mechanism 3. Roller extrusion and crushing mechanism 4. Secondary conveyor chain

Figure 1 Structure of film-soil conveying and vibration separation device

The working principle is shown in Figure 2. The digging device excavates the tillage soil and residual film, and throws them onto the first-level conveyor chain. Due to the use of soil clod excavation, the mixture on the first-level conveyor chain consists of finely fragmented soil, film-soil composite, and a small amount of fragmented residual film. The film-soil composite is a compact mass where residual film is tightly bonded with soil, meaning that the clods contain varying numbers of film layers. The residual film is irregularly distributed and shaped within the clods. The first-level conveyor chain moves the film-soil mixture backward, and the vibration mechanism designed below the conveyor chain vibrates, shaking off a large amount of finely fragmented soil into the field, thereby achieving the initial separation of the residual film and soil. The remaining film-soil composite and residual film are then transported to the roller compression and crushing mechanism, where the film-soil composite undergoes extrusion and crushing, completely separating the residual film from the soil clods. This further facilitates the separation of the soil and film. The separated residual film falls onto the secondary conveyor chain, and is then

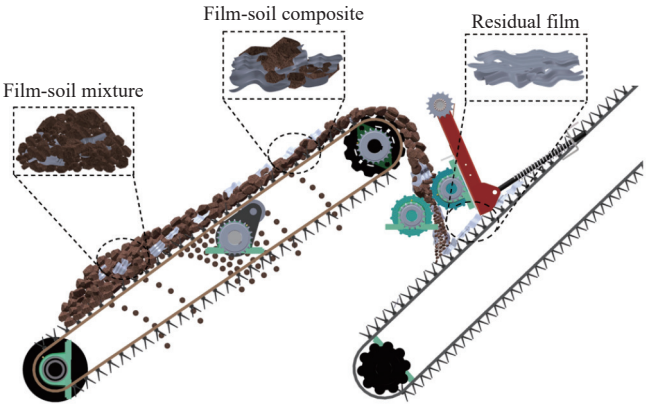

Figure 2 Working principle of film-soil mixture conveying and vibration separation device

gathered into a film collection box by the action of the film-removal rollers. Both conveyor chains are made of polyurethane flexible material, which has excellent elasticity and wear resistance, reducing the secondary fragmentation of the residual film caused by the "tearing" of the residual film.

3 Performance analysis of key components

3.1 Transport stability analysis of film-soil

When the film-soil mixture is thrown onto the first-level conveyor chain, the change in the speed and direction upon contact with the conveyor chain causes the film-soil composite to experience imbalanced phenomena such as rolling, sliding, and shifting. If the imbalance is severe, the film-soil composite may "jump" out of the machine, leading to film leakage. Based on the author's previous observations of the actual film-soil composite and high-speed camera recordings, when the film-soil composite falls onto the conveyor chain, it collides with the chain. The loosely bonded soil on the surface may break into finer particles and detach. Upon landing, the film-soil composite's velocity instantly synchronizes with the conveyor chain's movement. This process can be simplified as a transition from parabolic motion to linear motion after a deflection. During this deflection phase, the "edges" of the film-soil composite come into contact with the conveyor chain, creating friction that gradually rounds the composite into a more spherical shape. To clarify this mechanism, this section models the soil-film composite as an idealized spherical body for analysis. The contact between the film-soil composite and the first-level conveyor chain is divided into three stages: collision, sliding, and pure rolling. Kinematic analysis is conducted for each of these three stages.

3.1.1 Collision process analysis

Due to being ejected at high speed onto the first-level conveyor chain, and with its motion direction forming a certain angle with the conveyor chain, the relative speed of the film-soil composite on the conveyor chain is significantly higher than the speed of the conveyor chain itself. This leads to a tendency for rolling and sliding in the *x*-direction, as shown in Figure 3a.

3.1.2 Slip process analysis

Figure 3b illustrates the contact and sliding process between the film-soil composite and the conveyor chain. After the film-soil composite falls onto the conveyor chain, its lower end O_1 experiences a velocity difference with the conveyor chain. As a result, relative motion occurs between the two, and the conveyor chain generates a frictional force on the film-soil composite. During this stage, the film-soil composite undergoes decelerating motion until it transitions into pure rolling motion.

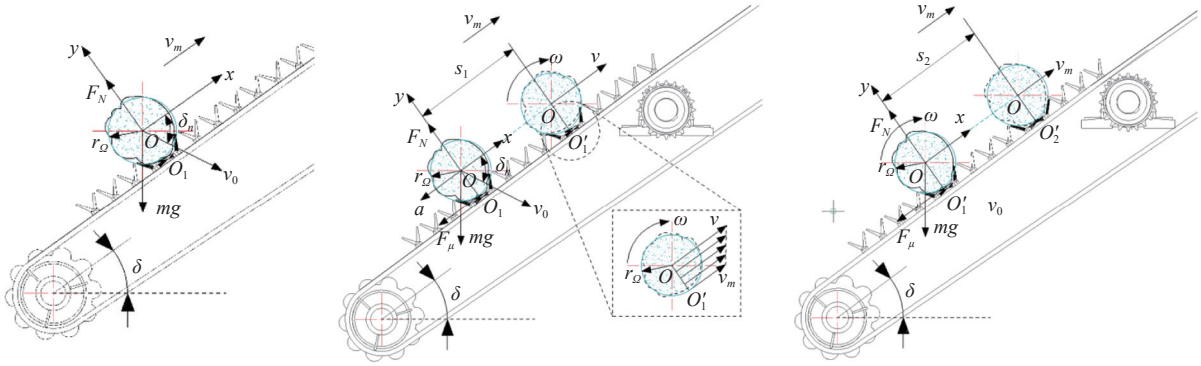

a. Vibrating mechanism b. Motion analysis of the slip process c. Pure rolling motion process

Figure 3 Conveying process of soil-film composite

Using the center of mass O of the film-soil composite as the origin, and establishing an *xoy*-coordinate system, the force analysis of the film-soil composite yields the following:

$$\begin{cases} ma = F_\mu + mg\sin\delta \\ J\sigma = F_\mu r_\Omega \\ F_N = mg\cos\delta \\ F_\mu = \mu F_N \\ J = \dfrac{1}{2}mr_\Omega^2 \end{cases} \tag{1}$$

where, F_μ denotes the frictional force exerted by the first-level conveyor chain on the film-soil composite, N; F_N denotes the supporting force of the conveyor chain on the film-soil composite, N; m denotes the mass of the film-soil composite, kg; r_Ω denotes the physical equivalent radius of the film-soil composite, m; δ denotes the conveying inclination angle of the conveyor chain, (°); a denotes the acceleration of the composite's center of mass, m/s²; J denotes the moment of inertia of the film-soil composite, kg·m²; μ denotes the coefficient of friction between the film-soil composite and the first-level conveyor chain, a constant; σ denotes the angular acceleration of the film-soil composite, r/min².

Solving the above equation gives the instantaneous acceleration a and angular acceleration σ as:

$$\begin{cases} a = \mu g\cos\delta + g\sin\delta \\ \sigma = \dfrac{2\mu g\cos\delta}{r_\Omega} \end{cases} \tag{2}$$

Based on kinematic principles, an analysis of the film-soil composite during this stage yields:

$$\begin{cases} s_1 = v_0 t_1\cos\delta_n - \dfrac{1}{2}at_1^2 \\ \omega = \alpha t_1 \\ v = v_0\cos\delta_n - at_1 \end{cases} \tag{3}$$

where, δ_n denotes the motion angle between the film-soil composite and the conveyor chain, (°); v denotes the center of mass velocity of the film-soil composite during pure rolling motion, m/s; ω denotes the angular velocity of the film-soil composite during pure rolling motion, r/min; s_1 denotes the maximum slip displacement of the film-soil composite during pure rolling motion, m; v_0 denotes the initial velocity of the film-soil composite when it falls onto the conveyor chain, m/s; t_1 denotes the slip time of the film-soil composite on the first-level conveyor chain, s.

Based on the analysis, when the contact point O' of the film-soil composite with the conveyor chain experiences friction from

the conveyor chain and decelerates to match the conveyor chain's running speed, the deceleration of the film-soil composite's center of mass velocity v will be less than the deceleration of the contact point velocity v_m. As a result, a velocity difference occurs between the center of mass O of the film-soil composite and the contact point O'. The film-soil composite will then undergo pure rolling on the conveyor chain. According to the instantaneous center of velocity method for planar motion, the following condition is satisfied:

$$v - v_m = \omega r_\Omega \tag{4}$$

where, v_m denotes the operating speed of the conveyor chain, m/s.

By substituting Equations (2) and (4) into Equation (3) and solving them simultaneously, the equations for the center of mass displacement, velocity, angular velocity, and time of the film-soil composite are obtained as follows:

$$s_1 = \frac{v_0^2\cos^2\delta_n - v_m v_0\cos\delta_n}{3\mu g\cos\delta + g\sin\delta} - \frac{v_m^2(\sin\delta+\mu\cos\delta)}{2g(3\mu\cos\delta+\sin\delta)^2} + \frac{v_0 v_m\cos\delta_n(\sin\delta+\mu\cos\delta)}{g(3\mu\cos\delta+\sin\delta)^2} - \frac{v_0^2\cos^2\delta_n(\sin\delta+\mu\cos\delta)}{2g(3\mu\cos\delta+\sin\delta)^2} \tag{5}$$

3.1.3 Pure rolling motion process analysis

Figure 3c illustrates the pure rolling process of the film-soil composite on the conveyor chain. As the film-soil composite continues to be transported upward, its angular velocity will gradually decrease until it becomes nearly stationary relative to the conveyor chain. At this point, the velocity of the film-soil composite's center of mass O is v_m. Only then will the film-soil composite begin to be transported smoothly.

To simplify the solution process, the entire conveyor system is considered a conservative system in this stage, with frictional energy losses within the system neglected. According to the theorem of kinetic energy, the following can be obtained:

$$\frac{1}{2}J\omega^2 + \frac{1}{2}mv^2 - \frac{1}{2}mv_m^2 = mgs_2\sin\delta \tag{6}$$

where, s_2 denotes the displacement of the film-soil composite during pure rolling motion on the first-level conveyor chain, m.

Substituting Equations (1) and (5) into Equation (6):

$$s_2 = \frac{v_m\mu\sin2\delta v_0\cos\delta_n - v_m^2\mu\sin2\delta}{g\sin\delta(3\mu\cos\delta+\sin\delta)^2} + \frac{3\mu^2\cos^2\delta v_0^2\cos^2\delta_n - 3v_m^2\mu^2\cos^2\delta}{g\sin\delta(3\mu\cos\delta+\sin\delta)^2} \tag{7}$$

From the above analysis, by combining Equations (5) and (7), the distance equation for stable transportation of the film-soil composite after it falls onto the first-level conveyor chain is obtained:

$$s = \frac{v_0^2\cos^2\delta_n - v_m v_0\cos\delta_n}{3\mu g\cos\delta + g\sin\delta} + \frac{b}{2g\sin\delta(3\mu\cos\delta+\sin\delta)^2} \tag{8}$$

where,

$$b = -v_m^2\sin^2\delta - 5v_m^2\mu\sin\delta\cos\delta + \left(2v_m\sin^2\delta + 3v_m\mu\sin2\delta\right)v_0\cos\delta_n + \left(6\mu^2\cos^2\delta - \sin^2\delta - \mu\sin\delta\cos\delta\right)v_0^2\cos^2\delta_n - 6v_m^2\mu^2\cos^2\delta$$

where, s denotes the distance traveled by the film-soil composite from landing on the first-level conveyor chain to the point where it moves synchronously with the first-level conveyor chain, m.

By analyzing the transportation process of the film-soil composite on the first-level conveyor chain, it can be determined that the main factors affecting its transportation stability are the conveyor chain speed v_m and the first-level conveyor chain inclination angle δ. During the transportation of the film-soil composite, the primary interaction is between the soil and the flexible conveyor chain. The reader may refer to the discussion on the first-level conveyor inclination angle in references[23,24], which related to the friction coefficient between soil and conveyor chain materials. Therefore, the first-level conveyor chain inclination angle is designed to be 25°. Further research is needed to study the impact of first-level conveyor chain speed on the stability of film-soil transportation.

3.2 Film-soil transport vibration mechanism

3.2.1 Component of the mechanism

The film-soil mixture ejected onto the first-level conveyor chain by the digging device mainly consists of a large amount of finely crushed soil, as well as film-soil composites and residual film. The presence of finely crushed soil increases the power consumption of the conveyor chain and causes blockages in the subsequent roller extrusion and crushing mechanism, leading to film leakage issues. To accelerate the falling of finely crushed soil to the field and achieve preliminary separation of the film-soil mixture, a vibrating mechanism for film-soil transportation is designed, as shown in Figure 4a.

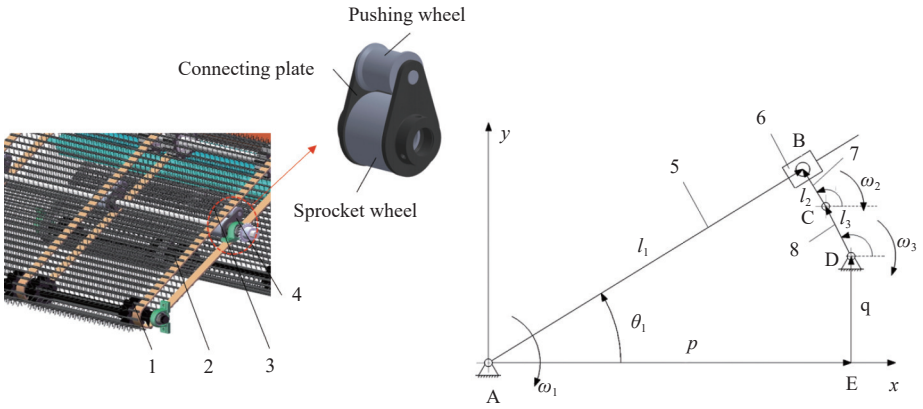

a. Vibrating mechanism b. Schematic diagram of the vibration mechanism motion analysis

Note: θ_1 is the position angle of guide rod, (°); θ_2 is the position angle of connecting rod, (°); θ_3 is the position angle of crank, (°); ω_1 is the rotational speed of guide rod, r/min; ω_2 is the rotational speed of connecting rod, r/min; ω_3 is the rotational speed of crank, r/min; l_1 is the length of AB section on guide rod, m; l_2 is the length of connecting rod, m; l_3 is the length of crank, m; p is the horizontal distance between vibration wheel and conveyor chain wheel, m; q is the vertical distance between vibration wheel and conveyor chain wheel, m.

1. Conveyor chain sprocket 2. Conveyor chain 3. Vibration wheel shaft 4. Vibration wheel 5.Guide rod 6. Slider 7. Connecting rod 8. Crank

Figure 4 Film-soil transport vibration system

The transport vibration system mainly consists of a conveyor chain sprocket, conveyor chain, vibration wheel shaft, and vibration wheels. The vibration wheel is composed of a push wheel, connecting plate, and a sprocket wheel. The principle is that the vibrating wheel is mounted on the vibrating wheel shaft. The vibrating wheel rotates clockwise, pushing the conveyor chain to produce a periodic vibration with alternating high and low amplitudes, which increases the disturbance of the film-soil composite during the conveying process, allowing fine soil to fall through the gaps in the conveyor chain.

3.2.2 Model establishment

To simplify the analysis, the flexibility of the conveyor chain is ignored, and the conveyor chain is treated as a rigid vibration rod. Studying the motion of the cam mechanism alone is relatively complex based on mechanical principles. This study simplifies the contact between the vibration wheel and the conveyor chain using the high-pair low-order method, transforming it into the contact between a guide rod and a slider. The entire vibration system is treated as a crank-slider mechanism, with the vibration rod being equivalent to guide rod 5, the drive chain wheel radius equivalent to connecting rod 7, and the center distance between the drive chain wheel and the support chain wheel equivalent to crank 8. The crank rotates clockwise. Using the analytical method, the motion parameters of the guide rod are obtained, and the vibration pattern of the conveyor chain is derived.

The position equation of the vibrating mechanism is established with point A as the origin. First, the vector directions for each component are drawn in Figure 4b. The angles θ_1, θ_2, and θ_3 of each component are drawn counterclockwise along the positive x-axis. Then, the vector equation is written by closing the loop ABCDE.

$$\vec{l}_1 = \vec{l}_2 + \vec{l}_3 + \vec{p} + \vec{q} \tag{9}$$

The vector equation can be written as a coordinate equation as follows:

$$\begin{cases} l_1 \sin\theta_1 - l_2 \sin\theta_2 - l_3 \sin\theta_3 = q \\ l_1 \cos\theta_1 + l_2 \cos\theta_2 + l_3 \cos\theta_3 = p \end{cases} \tag{10}$$

From the geometric relationship, it can be obtained that:

$$\theta_2 = \theta_1 + \frac{\pi}{2} \tag{11}$$

Bringing Equation (11) into Equation (10), and then differentiating with respect to time t, the result is:

$$\begin{cases} \dot{l}_1 \sin\theta_1 + l_1\omega_1 \cos\theta_1 + l_2\omega_1 \sin\theta_1 - l_3\omega_3 \cos\theta_3 = 0 \\ \dot{l}_1 \cos\theta_1 - l_1\omega_1 \sin\theta_1 - l_2\omega_1 \cos\theta_1 - l_3\omega_3 \sin\theta_3 = 0 \end{cases} \tag{12}$$

where, $\dot{l}_1$ denotes the relative velocity of the slider with respect to the guide rod, m/s.

The coordinate rotation method was employed to solve Equation (12), yielding the angular acceleration ε_1 of the guide rod and the relative acceleration $\ddot{l}_1$ of the slider with respect to the guide rod. It can be derived as follows:

$$\begin{cases} \varepsilon_1 = \dfrac{-l_2\omega_1^2 \cos 2\theta_1 - l_3\omega_3^2 \sin(\theta_3 + \theta_1)}{l_1 + l_2 \sin 2\theta_1} - \dfrac{2\dot{l}_1\omega_1}{l_1 + l_2 \sin 2\theta_1} \\ \ddot{l}_1 = \dfrac{-2\dot{l}_1\omega_1 l_2 \cos 2\theta_1 + l_1\omega_1^2 (l_1 + l_2 \sin 2\theta_1)}{l_1 + l_2 \sin 2\theta_1} - \dfrac{l_2\omega_1^2 l_1 \sin 2\theta_1 - M}{l_1 + l_2 \sin 2\theta_1} \end{cases} \tag{13}$$

where, ε_1 denotes the angular acceleration of the guide rod; $\ddot{l}_1$ denotes the relative acceleration of the slider with respect to the guide rod.

Namely,

$$M = -l_3\omega_3^2 [l_2 \sin(\theta_3 - \theta_1) - \cos(\theta_3 + \theta_1)] - l_2^2\omega_1^2$$

From the analysis of Equation (13), it can be seen that the angular velocity and angular acceleration of the guide rod are primarily determined by factors such as the crank speed ω_3, the distance l_1 between the point B and point A, as well as the lengths of the connecting rod l_2 and the crank l_3.

With reference to Figure 4, since the vibration wheel is a standard component, its structural parameters can be considered as non-influential factors. Therefore, to investigate the impact of the vibration wheel on film-soil separation, it is necessary to further explore the rotational speed of the vibration wheel and the distance between the vibration wheel and the front wheel of conveyor chain.

3.3 Analysis of the distribution height in the vibration conveying process of the film-soil mixture

This section primarily uses a high-speed camera to capture the film-soil mixture transport process on the conveyor chain. By altering the parameters of the vibration mechanism and repeatedly measuring the distribution height of the film-soil mixture during transport, the ability of the vibration mechanism to separate the film-soil mixture on the conveyor chain is assessed.

As shown in Figure 5, the distribution height of the film-soil mixture and the motion state of the film-soil composite at different moments on the conveyor chain are presented. The yellow dashed line represents the upper boundary of the film-soil mixture. Based on the analysis in Section 3.2.2, the key parameters of the vibration mechanism include the rotational speed of the vibration wheel and the installation distance between the vibration wheel and the front wheel of the conveyor chain. In order to explore the influence of factors on the film-soil separation effect of the conveyor chain vibration at different levels, so as to provide data for the field trials of the whole machine in the later stage, referring to the description of the potato conveyor chain in references [24] and [25] and the design size requirements of the whole machine of the plough layer residual film recovery machine, the rotational speed of the vibration wheel was preliminarily determined to be 150.0-220.0 r/min. The length of the conveyor chain is 1200.0 mm. The vibration wheel speed is set at five levels: 150.0, 167.5, 185.0, 202.5, and 220.0 r/min. The installation distance of the vibration wheel is set at five levels: 400.0, 562.5, 725.0, 887.5, and 1050.0 mm, as listed in Table 1. By varying the vibration wheel speed and installation distance, the distribution height of the film-soil mixture at different positions on the conveyor chain is observed. For convenience, the effective distance between the different positions on the conveyor chain and the front wheel is referred to as the “conveying length,” which is used to label the distribution height of the film-soil mixture at various points on the conveyor chain. For ease of experimental operation, mounting points for the vibration wheel were set at positions 400.0, 562.5, 725.0, 887.5, and 1050.0 below the conveyor chain to adjust the installation distance of the wheel.

3.3.1 Analysis of the impact of vibration wheel speed on film-soil mixture separation

Figure 6 shows the distribution height data of the film-soil mixture under different vibration wheel speed conditions when the vibration wheel installation distance is set to 725.0 mm. After further correction of the measured data, the resulting curve illustrates the variation in the distribution height of the film-soil mixture as a function of the conveying length.

a. 10 ms b. 15 ms c. 20 ms

Figure 5 Transport process of film-soil mixture

Table 1 Factors and levels of experiments

Levels	Vibration wheel rotational speed/r·min^{-1}	Installation distance/mm
1	150.0	400.0
2	167.5	562.5
3	185.0	725.0
4	202.5	887.5
5	220.0	1050.0

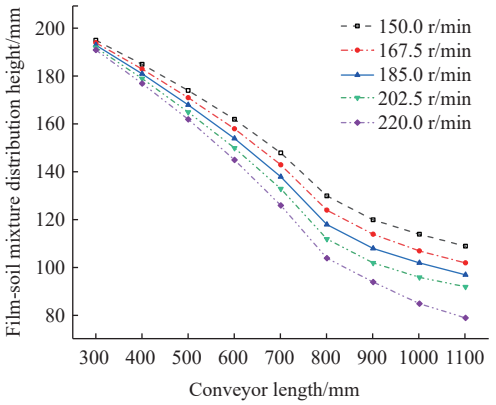

Figure 6 Influence of cam speed on separation of film-soil mixture

From Figure 6, it can be observed that when the vibration wheel speed is within the range of 167.5, 185.0, and 202.5 r/min, at a conveying length of 1100.0 mm, the height of the film-soil mixture remains between 90.0 and 110.0 mm, indicating that most of the finer soil in the film-soil mixture has already fallen to the field, leaving only the film-soil composite and residual film on the conveyor chain. When the vibration wheel speed is 150.0 r/min, the height of the film-soil mixture at the 1100.0 mm position is greater than 110.0 mm, indicating that some finer soil has not yet fallen to the field. When the vibration wheel speed is 220.0 r/min, the height of the film-soil mixture at the 1100.0 mm position continues to decrease, which is due to the excessive vibration wheel speed causing the film-soil composite to "jump" out of the machine.

3.3.2 Analysis of the effect of vibration wheel installation distance on film-soil mixture separation

Figure 7 shows the distribution height data of the film-soil mixture under different vibration wheel installation distance conditions when the vibration wheel speed is set to 185.0 r/min. After further correction of the measured data, the resulting curve illustrates the variation in the distribution height of the film-soil mixture as a function of the conveying length.

It can be observed that different vibration wheel installation positions result in varying degrees of reduction in the height of the film-soil mixture in Figure 7. However, from the perspective of the separation efficiency of the film-soil mixture by the conveyor chain, when the vibration wheel installation distance is 400.0 mm or 1050.0 mm, the height of the film-soil mixture at a conveying length of 1100.0 mm remains between 110.0 and 120.0 mm, significantly higher than when the installation distances are 562.5 mm, 725.0 mm, or 887.5 mm. This suggests that finer soil has not yet been fully separated and dropped off the conveyor chain. Therefore, when the vibration wheel installation distance is either too large or too small, the vibration effect on the conveyor chain is not significant.

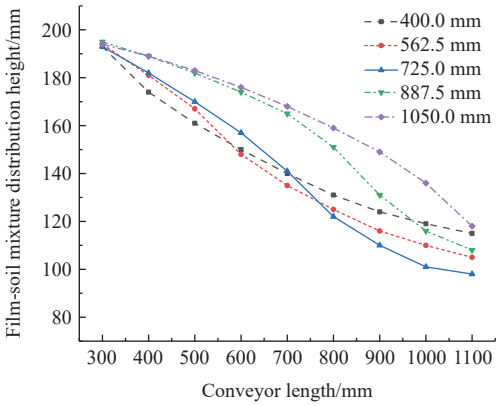

Figure 7 Effect of installation distance on separation of film-soil mixture

In conclusion, based on the analysis, when the vibration wheel speed is between 167.5 r/min and 205.5 r/min and the installation distance is between 562.5 mm and 887.5 mm, the separation of the film-soil mixture is more pronounced. This range can be used as the experimental parameter values to further investigate the film-soil separation process.

3.4 Roller extrusion and crushing mechanism

The roller extrusion and crushing mechanism primarily consists of components such as crushing roller 1, crushing roller 2, rocker arm, pressing rod, and reset spring, with a certain gap left between the two crushing rollers. This mechanism uses a pair of crushing rollers to separate fine soil from the conveyor chain, then compress and crush the remaining film-soil composite, allowing the residual film to be separated from the agglomerated soil, thus achieving film-soil separation. The residual film, being a flexible material, can pass through the gap between the two crushing rollers, preventing secondary film shredding, as shown in Figure 8.

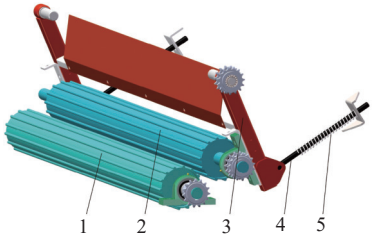

1. Crushing roller 1 2. Crushing roller 2 3. Rocker arm 4. Pressing rod 5. Reset spring

Figure 8 Roller extrusion and crushing mechanism

As shown in Figure 9a, when the film-soil composite falls onto the roller extrusion and crushing mechanism, the two crushing rollers make contact with the film-soil composite and rotate in opposite directions, compressing and crushing the film-soil composite. The forces equations for the film-soil composite can be established as follows:

$$\begin{cases} G+\left(N_f+N_{f1}\right)\cos\varphi-(F_{\mathrm{N}}+F_{\mathrm{N1}})\sin\varphi\geq 0 \\ N_f=fF_{\mathrm{N}} \\ N_{f1}=fF_{N1} \\ F_{\mathrm{N}}=F_{N1} \end{cases} \tag{14}$$

where, f denotes the coefficient of friction between the film-soil composite and the crushing rollers.

From the analysis of Figure 9a, it can be seen that the compression and crushing of the film-soil composite mainly occurs due to the shear force formed in the x-direction after the two crushing rollers contact the composite. This shear force shears and breaks the agglomerated soil.

As shown in Figure 9b, the shear action formed when the two crushing rollers contact the film-soil composite is illustrated. At the moment of contact between the film-soil composite and the crushing rollers, it can be equivalently modeled as a shear force F_s acting on a cylindrical beam with a shear length dy and a shear area A. The crushing of the film-soil composite mainly occurs due to the shear force F_s acting on the cylindrical beam. This causes a small bending deformation in the cylindrical beam. When the bending deformation accumulates to a certain extent, the cylindrical beam will fracture, which results in the film-soil composite breaking apart.

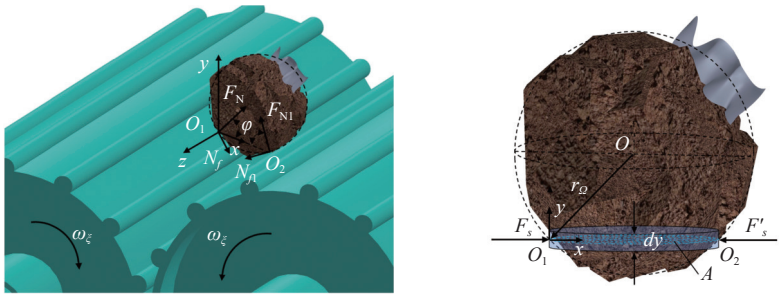

a. Forces analysis of film-soil composite b. Shear stress on the film-soil composite

Note: O_1 denotes the left collision contact point between the crushing roller and the film-soil composite; O_2 denotes the right collision contact point between the crushing roller and the film-soil composite; F_{N} and F_{N1} denote the support forces exerted by the crushing rollers on the film-soil composite, N; φ denotes the angle between the support force and the x-axis of the coordinate system, in degrees (°); N_f and N_{f1} denote the frictional forces exerted by the crushing rollers on the film-soil composite, N; ω_ξ denotes the rotational speed of the crushing rollers, r/min; F_s denotes the shear force formed by the crushing rollers acting on the film-soil composite, N; A denotes the area of the film-soil composite being sheared, m^2.

Figure 9 Extrusion analysis of membrane soil complex by the mechanism

Based on Figure 9, we can use the following relationships:

$$F_s=F_{\mathrm{N}}(\cos\varphi+f\sin\varphi) \tag{15}$$

From the geometric relationship, the shear area A is given by:

$$A=\pi r_\Omega^2\cos^2\varphi \tag{16}$$

According to the principles of materials mechanics, when the cross-section of a beam is circular, it cannot be assumed that the shear stresses at all points on the cross-section are parallel to the shear force F_s. By applying the Tresca yield criterion, the maximum shear stress $\tau_{\max}$ is given by:

$$\tau_{max}=\frac{4F_s}{3A} \tag{17}$$

By solving Equations (14) to (17) simultaneously, we obtain:

$$\tau_{\max}=\frac{4F_{\mathrm{N}}(\cos\varphi+f\sin\varphi)}{3\pi r_\Omega^2\cos^2\varphi}\leq\frac{2(\cos\varphi+f\sin\varphi)G}{3(\sin\varphi-f\cos\varphi)\pi r_\Omega^2\cos^2\varphi} \tag{18}$$

The film-soil composite needs to satisfy the following condition for being crushed by the crushing rollers:

$$\tau_{\max}\geq[\tau] \tag{19}$$

where, $[\tau]$ denotes the allowable shear stress of the film-soil composite, kPa.

The average weight of the film-soil composite G is measured to be approximately 27.73 N, and the maximum equivalent radius r_Ω of the film-soil composite is 0.046 m. Xinjiang's soil is sandy, with a moisture content ranging from 15% to 22%, and the maximum shear stress of the soil is 12.3 kPa. The coefficient of friction between the soil and steel f is 0.2, and the angle between the supporting force F_{N} of the soil-crushing rollers and the horizontal axis is 46°. Based on Equation (18), the maximum shear stress $\tau_{\max}$ is calculated to be 63.86 kPa, which is greater than the maximum shear stress of the film-soil composite. This satisfies Equation (19) and meets the design requirements.

4 Experiment and analysis

4.1 Experimental materials

To verify the accuracy of the theoretical analysis, assess the performance of the device, and identify the optimal parameter combinations, a field experiment was conducted in November 2023 at a cotton planting base in Yuli County, Mongolian Autonomous Prefecture of Bayingolin, Xinjiang (84°02′E, 40°10′N). The experimental field had been used for cotton cultivation with film-covered planting for 10 consecutive years, with a soil moisture content of 19.2% and an area of 100 acres. The test equipment included a John Deere 2004 model tractor with a power output of 200.9 kW. Field operation conditions are shown in Figure 10.

a. Test process b. Test effect

Figure 10 Field trial

4.2 Experimental methods

Using soil content rate and film leakage rate as evaluation indicators, the performance of the film-soil conveying and vibration separation device is assessed. The calculation formulas are as follows:

$$Y_1 = \left(1 - \frac{m_1}{M}\right) \times 100\% \tag{20}$$

$$Y_2 = \frac{m_2}{m_1 + m_2} \times 100\% \tag{21}$$

where, Y_1 denotes the soil content rate, %; Y_2 denotes the film leakage rate, %; m_1 denotes the mass of the recovered residual film from the tillage layer, kg; m_2 denotes the mass of the residual film that falls to the ground after recovery, kg; M denotes the total mass of the film-soil mixture recovered in the experiment, kg.

Based on the theoretical analysis of the conveying and separation process, a three-factor, three-level experiment was conducted, selecting the conveyor chain speed, vibrating wheel rotation speed, and the installation distance between the front wheel of the first-level conveyor chain and the vibrating wheel as the three factors. According to the research on potato-soil vibration transport in references [24, 25], when the first-stage conveyor chain speed ranges from 0.8 to 2.4 m/s, the soil separation is significant, which serves as the range for this factor. Based on the analysis in Section 2.3, the vibration wheel speed is set between 167.5 and 202.5 r/min, and the installation distance is set between 562.5 and 887.5 mm.

The experiment was conducted using a three-factor, three-level Box-Behnken response surface methodology[26], with the factor coding listed in Table 2.

4.3 Variance and discussion

4.3.1 Analysis of variance

Each experimental group was repeated five times to calculate the average values of soil content rate and film leakage rate, resulting in the experimental outcomes presented in Table 3.

Variance analysis of the experimental results was performed using Design-Expert 8.0.6 software, with the results as listed in Table 4.

Table 2 Factors and codes of experiments

Coding table	Conveyor chain speed X_1/m·s^{-1}	Vibrating wheel rotation speed X_2/r·min^{-1}	Installation distance X_3/mm
–1	0.80	167.5	562.5
0	1.60	185.0	725.0
1	2.40	202.5	887.5

Table 3 Test plan and experimental results

Test No.	X_1/m·s^{-1}	X_2/r·min^{-1}	X_3/mm	Y_1/%	Y_2/%
1	0.80	167.5	725.0	29.93	10.76
2	2.40	167.5	725.0	26.80	10.59
3	0.80	202.5	725.0	27.61	11.42
4	2.40	202.5	725.0	19.56	16.65
5	0.80	185.0	562.5	26.63	12.91
6	2.40	185.0	562.5	24.33	19.83
7	0.80	185.0	887.5	29.74	13.78
8	2.40	185.0	887.5	18.17	13.45
9	1.60	167.5	562.5	24.90	13.75
10	1.60	202.5	562.5	23.34	14.93
11	1.60	167.5	887.5	24.62	11.86
12	1.60	202.5	887.5	18.83	12.25
13	1.60	185.0	725.0	18.60	9.11
14	1.60	185.0	725.0	18.03	10.11
15	1.60	185.0	725.0	19.49	8.24
16	1.60	185.0	725.0	18.59	10.39
17	1.60	185.0	725.0	19.44	9.09

Table 4 Variance analysis of soil content rate and film leakage rate

Source	Soil content rate					Film leakage rate				
	Sum of squares	DF	Mean square	F-value	p-value	Sum of squares	DF	Mean square	F-value	p-value
Model	287.71	9	31.97	64.83	< 0.0001**	133.47	9	14.83	15.43	0.0008**
X_1	78.44	1	78.44	159.07	< 0.0001**	16.97	1	16.97	17.65	0.0040**
X_2	35.74	1	35.74	72.49	< 0.0001**	8.59	1	8.59	8.94	0.0202*
X_3	7.68	1	7.68	15.58	0.0056**	12.70	1	12.70	13.21	0.0083**
X_1X_2	6.05	1	6.05	12.27	0.0099**	7.29	1	7.29	7.59	0.0283*
X_1X_3	21.48	1	21.48	43.57	0.0003**	13.14	1	13.14	13.67	0.0077**
X_2X_3	4.47	1	4.47	9.07	0.0196*	0.16	1	0.16	0.16	0.6990
X_1^2	84.13	1	84.13	170.62	< 0.0001**	23.87	1	23.87	24.84	0.0016**
X_2^2	30.13	1	30.13	61.10	0.0001**	1.45	1	1.45	1.50	0.2596
X_3^2	8.46	1	8.46	17.16	0.0043**	43.75	1	43.75	45.52	0.0003**
Residual	3.45	7	0.49			6.73	7	0.96		
Lack of fit	1.89	3	0.63	1.62	0.3186	3.72	3	1.24	1.65	0.3134
Pure error	1.56	4	0.39			3.01	4	0.75		
Cor total	291.16	16				140.20	16			

Note: p<0.01 means extremely significant**; 0.01<p<0.05 means very significant*. *DF*: Degree of freedom.

From Table 4, it can be seen that the p-values for the regression models of soil content rate and film leakage rate are both less than 0.01, indicating that the fitting models for both evaluation indicators are highly significant. The p-values for the lack of fit terms are greater than 0.05, which are not significant, suggesting that the equation provides a good model fit. The factors affecting the residual film-soil content rate, in descending order of influence, are X_1, X_2, and X_3, with interaction effects ranked as X_1X_3, X_1X_2, and X_2X_3. For the film leakage rate, the factors affecting it, in descending order, are X_1, X_3, and X_2, with interaction effects ranked as X_1X_3 and X_1X_2. The R^2 values for the two models are 0.9881 and 0.9520, indicating that they can be used for predicting soil content rate and film leakage rate, respectively.

4.3.2 Response surface analysis

To understand the interaction effects of the experimental factors on the soil content rate and film leakage rate, the Design-Expert 8.0.6 software was used to plot the response surface diagrams for soil content rate and film leakage rate, as shown in Figure 11.

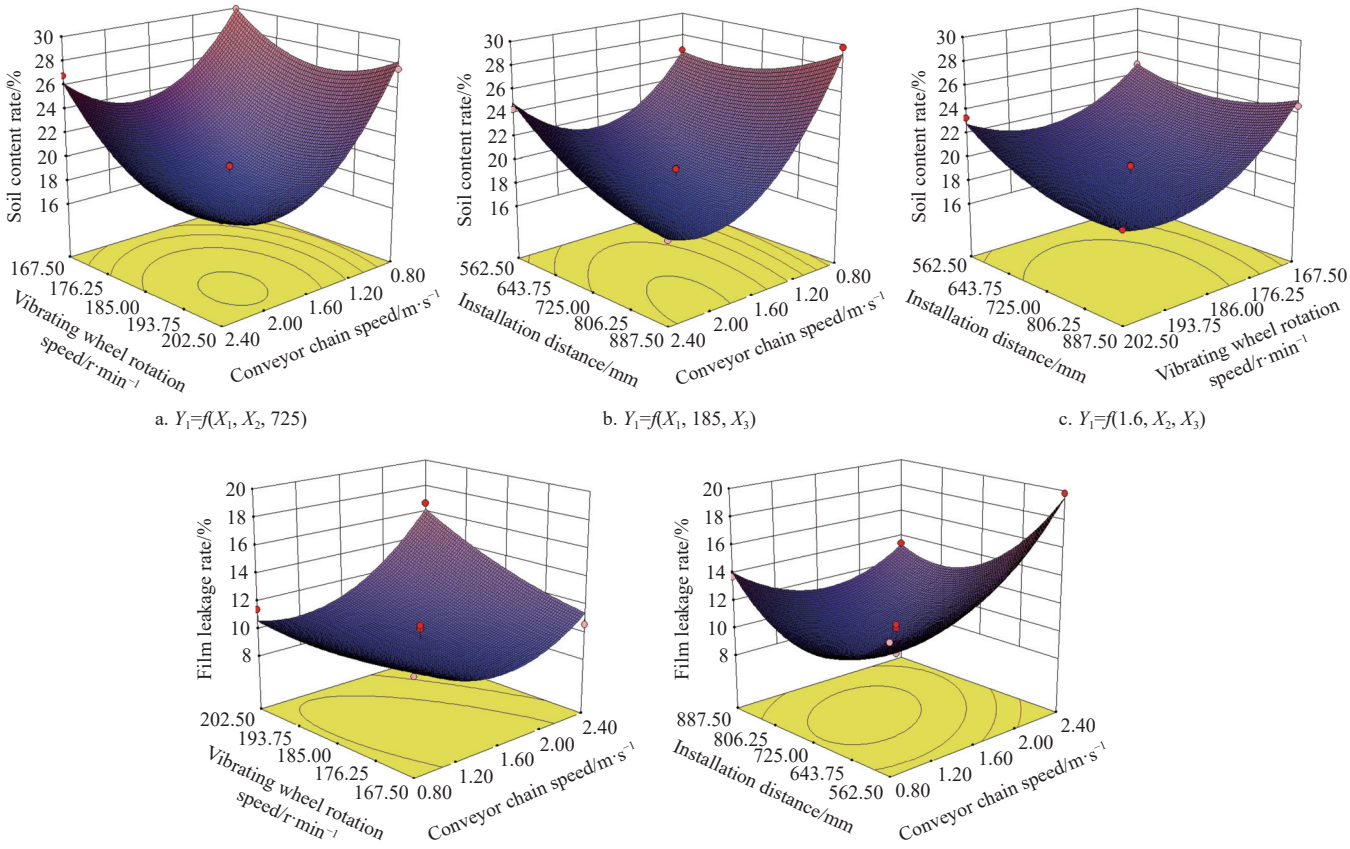

a. $Y_1=f(X_1, X_2, 725)$ b. $Y_1=f(X_1, 185, X_3)$ c. $Y_1=f(1.6, X_2, X_3)$

d. $Y_2=f(X_1, X_2, 725)$ e. $Y_2=f(X_1, 185, X_3)$

Figure 11 Response surface of influence of interaction of test factors on indicators

From Figures 11a-11c, it can be observed that the pairwise interactions of the three factors have different degrees of impact on the soil content rate. Additionally, as the conveyor chain speed increases, the soil content rate of the residual film first decreases and then increases, reaching a minimum value around 1.6 m/s. Similarly, as the vibration wheel speed increases, the soil content rate first decreases and then increases, with the minimum occurring around 189.6 r/min. The soil content rate also decreases and then increases as the installation position changes.

From Figure 11d, it can be seen that as the conveyor chain speed increases, the film leakage rate initially slightly decreases and then gradually increases. This trend is most pronounced during the increase in vibration wheel speed. Moreover, as shown in Figure 11e, the film leakage rate decreases and then increases with the increase in installation distance. This trend is also influenced by the conveyor chain speed: the smallest variation in trend occurs when the conveyor chain speed is at its minimum, and the largest variation occurs when the conveyor chain speed is at its maximum.

4.4 Parameter optimization

To obtain the optimal operational parameters for recovering the residual film from the cultivated layer, the Optimization module of Design-Expert 8.0.6 software is used to perform optimization of the regression model with constrained objectives[27]. The optimization goals are to minimize the soil content rate and the film leakage rate. The optimization objective function is defined as follows:

$$P = \begin{cases} \min Y_1(X_1,\ X_2,\ X_3) \\ \min Y_2(X_1,\ X_2,\ X_3) \end{cases} \tag{22}$$

Constraint function as:

$$\text{s.t} \begin{cases} 0.8\ \text{m/s} \le X_1 \le 2.4\ \text{m/s} \\ 180\ \text{r/min} \le X_2 \le 205\ \text{r/min} \\ 530\ \text{mm} \le X_3 \le 910\ \text{mm} \end{cases} \tag{23}$$

The analysis shows that when the conveyor chain speed is 1.6 km/h, the vibration wheel speed is 189.7 r/min, and the installation distance is 769.7 mm, the soil content rate is 18.31%, and the film leakage rate is 9.49%, with a confidence level of 95.9%.

4.5 Experimental verification

To verify the correctness of the optimized parameter combination, the conveyor chain speed of 1.6 km/h, vibration wheel speed of 189.7 r/min, and installation distance of 769.7 mm were selected for the validation experiment. Each experiment was repeated five times, and the average value was taken as the final result. The validation test results showed that the soil content rate was 19.11% and the film leakage rate was 10.12%, with error values of 4.36% and 6.63%, respectively. The performance evaluation indicators of the film-soil separation device were within the optimized range, confirming the reliability of the optimized combination.

5 Conclusions

1) Based on the current situation of mechanical recovery of residual film in the plough layer in Xinjiang, a film-soil separation device for recovering residual film from the cultivated layer was designed using the “vibration conveyor + double rollers + conveyor” mechanical method. This device successfully completes the vibration transportation of the film-soil mixture and the crushing of the film-soil composite, achieving the recovery of residual film in the plough layer.

2) A study was conducted on the transportation process of the film-soil composite, analyzing the collision stage, sliding stage, and pure rolling stage. It was found that the key factor affecting the stability of the film-soil composite's transport was the conveyor chain speed.

3) A vibration mathematical model for the conveyor chain was established, and the relationship between the vibration mechanism parameters and vibration characteristics was analyzed. It was found that the influencing factors were the vibration wheel speed and installation distance. Using high-speed cameras, the distribution height of the film-soil mixture on the conveyor chain was analyzed. The effects of different vibration wheel speeds and installation distances on film separation were determined, and the range of vibration wheel speeds and installation distances was established.

4) The double-roller crushing mechanism was designed, and a crushing force model was developed. Using the third-strength theory, the crushing mechanism of the film-soil composite was clarified, achieving efficient separation of the film and soil.

5) A field test was conducted with three factors: conveyor chain speed, vibration wheel speed, and installation position. Soil content rate and film leakage rate were selected as experimental indicators. A regression model between the experimental indicators and influencing factors was established, and optimization was performed. The optimal combination was found to be a conveyor chain speed of 1.6 km/h, a vibration wheel speed of 189.7 r/min, and an installation distance of 769.7 mm. At this combination, the soil content rate was 18.31%, and the film leakage rate was 9.49%. Field test verification showed that the error values for the experimental indicators were 4.36% and 6.63%, respectively, which met the operational requirements.

Acknowledgements

This work was supported by the Science and Technology Innovation Leading Talent Project (Grant No. 2024TSYCLJ0014), the Xinjiang Agricultural Machinery R&D Manufacturing Promotion and Autonomous Region Graduate Research Innovation Project (Grant No. XJ2024G103), the Xinjiang Uygur Autonomous Region "Unveiling and Leading" Project "High-Quality and High-Efficiency Mechanized Recovery Technology R&D and Equipment Application for Farmland Plastic Film Residue", and the Xinjiang Uygur Autonomous Region "Unveiling and Leading" Project (Grant No. XJJBGS-MG202403).

[References]

[1] Jiang D L, Yan L M, Chen X G, Mo Y S, Yang J C. Design and experiment of nail tooth picking up device for strip type residual film recycling and baling machine. Int J Agric & Biol Eng, 2023; 16(6): 85–96.

[2] Wang D W, Wang Z H, Ding H W, Zhou B, Zhang J Z, Li W H, et al. Effects of biodegradable mulching films on soil hydrothermal conditions and yield of drip-irrigated cotton (*Gossypium hirsutum* L.). Int J Agric & Biol Eng, 2022; 15(6): 153–164.

[3] Liang R Q, Zhang B C, Chen X G, Meng H W, Wang X Z, Shen C J, et al. Design and test of a multi-edge toothed cutting device for membrane-impurity mixed material. Int J Agric & Biol Eng, 2023; 16(2): 73–84.

[4] Shi Z L, Zhang X J, Liu X P, Guo L, Zhang C S, Liu L. Design and test of roll-type tillage layer residual film recovery machine. Transactions of the CSAM, 2024; 55(2): 128–137. (in Chinese)

[5] Ren Y, Guo W S, Wang X F, Hu C, Wang L, He X W, et al. Separation and mechanical properties of residual film and soil. Int J Agric & Biol Eng, 2023; 16(1): 184–192.

[6] Liu X L, Zhao W Y, Zhang H, Wang G P, Sun W, Dai F, et al. Design and experiment of an upper-side-discharge straw-returning and bundle self-unloading integrated corn residual film recycling machine. Int J Agric & Biol Eng, 2023; 16(5): 61–70.

[7] Yuan P P, Li H W, Lu C Y, Wang Q J, He J, Huang S H, et al. Design and experiment of seed furrow cleaning device based on throwing and sliding for no-till maize seeding. Int J Agric & Biol Eng, 2022; 15(4): 95–102.

[8] Dai F, Wang F, Guo W J, Shi R J, Xin S L, Liu X L, et al. Simulation and test on the operation process of an intermittent film-picking component on full-film mulched double ditches. Int J Agric & Biol Eng, 2024; 17(1): 99–108.

[9] Niu W Q, Zou X Y, Liu J J, Zhang M Z, Lu W, Gu J. Effects of residual plastic film mixed in soil on water infiltration, evaporation and its uncertainty analysis. Transactions of the CSAE, 2016; 32(14): 110–119. (in Chinese)

[10] Zhang Z Y, Li J B, Wang X F, Zhao Y M, Xue S K, Su Z P, et al. Design and test of 1SMB-3600A type fragmented mulch film collector for sowing layer soil. Soil & Tillage Research, 2022; 225: 105555.

[11] Guo W S, Hu C, He X W, Wang L, Hou S L, Wang X F. Construction of virtual mulch film model based on discrete element method and simulation of its physical mechanical properties. Int J Agric & Biol Eng, 2020; 13(4): 211–218.

[12] Guo H, Yu X D, Jin W, He N D, Guo W H. Establishment of prediction model for tensile mechanics of plastic film and prediction of film thickness. Journal of Chinese Agricultural Mechanization, 2020; 41(1): 173–178. (in Chinese)

[13] Zhang J X, Wang X N, Zhang L, Yu C, Jiang Y X, Zhang H C, et al. Effects of mechanical tensile properties of plastic film on plastic recycling method. Transactions of the CSAE, 2015; 31(20): 41–47. (in Chinese)

[14] Hu C, Wang X F, Wang S G, Lu B, Guo W S, Liu C J, et al. Impact of agricultural residual plastic film on the growth and yield of drip-irrigated cotton in arid region of Xinjiang, China. Int J Agric & Biol Eng, 2020; 13(1): 160–169.

[15] Zhang Z Y, Li J B, Wang X F, Zhao Y M, Xue S K, Su Z P. Parameters optimization and test of an arc-shaped nail-tooth roller-type recovery machine for sowing layer residual film. Agriculture, 2022; 12(5): 660.

[16] Zhang Z Y, Chen X G, Wang X F, Xue S K, Li J B. Design and test of the arc-shaped nail-tooth roller residual film recovery machine from the sowing layer. Int J Agric & Biol Eng, 2024; 17(1): 90–98.

[17] Zhang X J, Liu J Q, Shi Z L, Jin W, Yan J S, Yu M J. Design and parameter optimization of reverse membrane and soil separation device for residual film recovery machine. Transactions of the CSAE, 2019; 35(4): 46–55. (in Chinese)

[18] Guo W S, He X W, Wang L, Zhao P F, Hu C, Hou S L, et al. Development of a comb tooth loosening and pneumatic stripping plough layer residual film recovery machine. Transactions of the CSAE, 2020; 36(18): 1–10. (in Chinese)

[19] Luo K, Yuan P P, Jin W, Yan J S, Bai S H, Zhang C S, et al. Design of chain-sieve type residual film recovery machine in plough layer and optimization of its working parameters. Transactions of the CSAE, 2018; 34(19): 19–27. (in Chinese)

[20] Zhang Z H. Design and research of the air separation type reclaimer for the residual film of plough layer. Shanxi Agricultural University, 2020. (in Chinese)

[21] Shen S L, Zhang J X, Jiang Y X, Wang Y C, Liu X F, Li J M, et al. Tensile properties of residual film in tillage layer based on discrete element method. Transactions of the CSAM, 2024; 55(7): 132–141. (in Chinese)

[22] Yao J T, Zhang X J, Shi Z L, Liu X P, Kang M C, Guo L. Research status and development trend of tillage layer residual film recycling machine. Journal of Chinese Agricultural Mechanization, 2024; 45(8): 290–295. (in Chinese)

[23] Yang R B, Tian G B, Shang S Q, Wang B J, Zhang J, Zhai Y M. Design and experiment of roller group type potato soil separator for potato harvester. Transactions of the CSAM, 2023; 54(2): 107–118. (in Chinese)

[24] Lü J Q, Yang X H, Lu Y N, Li Z H, Li J C, Du C L. Analysis and experiment of potato damage in process of lifting and separating potato excavator. Transactions of the CSAM, 2020; 51(1): 103–113. (in Chinese)

[25] Lü J Q, Sun H, Dui H, Peng M M, Yu J Y. Design and experiment on conveyor separation device of potato digger under heavy soil condition. Transactions of the CSAM, 2017; 48(11): 146–155. (in Chinese)

[26] Liang R Q, Chen X G, Jiang P, Zhang B C, Meng H W, Peng X B, et al. Calibration of the simulation parameters of the particulate materials in film mixed materials. Int J Agric & Biol Eng, 2020; 13(4): 29–36.

[27] Hou S Y, Wang S Z, Zhu X X, Zhang J C, Ji W Y, Chen H T. Design and experiment of side-open sliding cutting film broken seeding unit based on straw fiber film. Transactions of the CSAM, 2021; 52(10): 155–165. (in Chinese)